Evaluating the Effect of Initial Gravity Forces in Buckling-Restrained Brace Frame Braces.

B. Saxey, C.H. Li
CoreBrace, West Jordan, USA.

Rafael Sabelli
Walter P. Moore, San Francisco, USA.

ABSTRACT

It is common practice to design buckling-restrained braces (BRBs) for seismic forces only, and to neglect any initial gravity that occurs in them. This practice assumes that these gravity loads simply "shed" upon first yielding of the braces, with negligible effect on the brace or system performance. This study investigates the case of a 12-story building, comparing the performances of braces designed neglecting initial gravity loads with those that include it.

Accounting for initial gravity forces in BRBs will result in increased member sizes. As it is generally understood that a stronger lateral system leads to better performance, the proof of the necessity of a potential design requirement must be distinguished from the beneficial effect of simply increasing member size at the expense of structural cost. For this purpose, the study considers designs including and excluding brace gravity forces, and also has conditions with gravity load present on the frame and conditions with frame gravity load moved incrementally to a P-Delta column. Thus, the difference in performance between lateral systems of different strengths can be compared with the difference in performance (if any) between conditions with and without initial brace gravity forces. The systems will be analysed with nonlinear response history analysis (NLRHA) to investigate the effects of the different systems within the study with the goal of eliminating unnecessary expense in the structural design. Results will be compared based on the metrics of brace ductility demand and lateral story drift.

1 INTRODUCTION

Common design practice for designing buckling-restrained braced frames (BRBF) assigns all gravity forces to the frame members and all lateral forces to the BRB members. In the elastic range of response, both of these forces would be shared by the frame and the BRBs based on the relative rigidity of each. For seismic forces, assuming that all the load is taken by the BRB is conservative for brace design since frame members are not relied upon to take lateral loads, and in many configurations the lateral load that would be proportioned to the frame is very small. The amount of gravity force that would be taken by the BRB member is dependent on the stiffness and angle of the BRB and the stiffness of the beams and columns and may not be small. While the loads that could be assigned to the BRB from a stiffness analysis can be significant, the frame members are required by ANSI/AISC 341 (AISC, 2022) to be designed for 100% of this load, plus the vertical component of the BRB, and upon yielding of the BRB its stiffness will be reduced such that gravity loads will be taken almost entirely by the frame members, and as such, the gravity loads in the BRB members are only present only while they are elastic. Based on these two points, it has become common to neglect gravity loads in sizing BRBs.

Designing the BRB for seismic-only forces is a design simplification that allows the quick and straightforward sizing of the BRB members without the need for a relative rigidity analysis to be performed to distribute gravity loads between the frame and the BRB. Several software packages exist, however, that will perform this stiffness analysis for the user. When such an analysis is performed, the BRB is sized for the full seismic forces plus some portion of the vertical gravity loads, resulting in larger BRB sizes. The frame members, in turn, have a smaller pre-yield demand, but must be designed for the vertical component of the capacity-based seismic demand of the, now larger, BRB, plus the full vertical component of the gravity load. Thus, accounting for the sharing of gravity loads in BRBF design, this will lead to larger BRB member sizes and larger axial forces in frame members (and thusly larger members) when capacity-based design prescriptions are followed. The effect, for the resulting capacity-based design, is identical to selecting a smaller R-factor.

2 DESIGN OF MODEL BUILDING ARCHETYPE

To investigate the significance of including the sharing of gravity loads in BRBF analysis, a 12-story BRBF building was considered. The design of this structure was adapted from NIST GCR 10-917-8 report (NIST, 2010; see Appendix C). A typical floor plan of the structure is shown in Figure 1(a) and a typical elevation of the BRBF with 2-story X-bracing configuration is given in Figure 1(b). The building structure (referred to as the NIST building in this study), per the NIST report, had a roof dead load (DL) of 327 kg/m², a floor DL of 415 kg/m², a roof live load (LL) of 98 kg/m², and a floor LL of 244 kg/m². The curtain wall weight considered was 73 kg/m². The spectral accelerations, S_{DS} and S_{D1}, used for seismic design were 1.0g and 0.6g, respectively, according to the NIST report.

In this study, a single perimeter BRBF, which carries ¼ seismic weight of the entire building, aligned in the longitudinal direction of the NIST building is taken as the example BRBF see Figure 1(a). The gravity loads tributary to this perimeter BRBF based on the NIST building condition is considered as a unit of "local gravity load" for the BRBF design. Figure 2 illustrates the four design cases considered in this study. The four cases are divided into two groups based on the amount of gravity loads used in the BRBF design. The two gravity load conditions considered are "one times (1x)" and "two times (2x)" local gravity load, which can be thought respectively to represent the gravity load effects on a BRBF located at the perimeter and in an interior frame of the building. Specific gravity loads used in the design include the point loads acting the BRBF columns (P_{GC}) and uniformly distributed loads (w_{GB}) on the BRBF beams. Note that this uniform beam load comes from curtain wall weight in combination with a fictitious distributed load representing an equivalent total load of the original point loads, coming from the transvers floor beams, acting on the 1/3 span of the BRBF beams.

Within each gravity load case group, two BRBF design methods, based on different approaches of brace sizing, were conducted, in which the braces were sized for earthquake effect only in the first case, and for combination of seismic and gravity effects in the second case. These two cases are named "E-Only" and

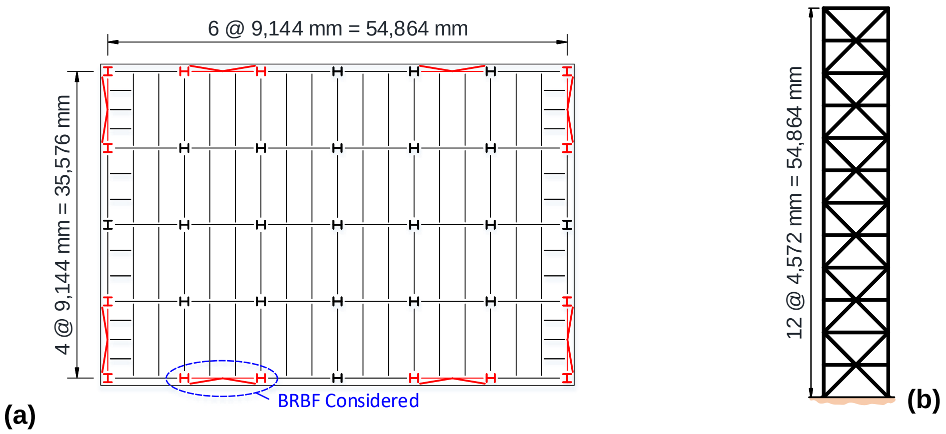

Figure 1: Twelve-story NIST building archetype: (a) floor plan and (b) elevation of BRBF.

"E+G", respectively, and, along with the two gravity load cases, result in four design cases in total. The four design cases are named $P_{E,1}$, $P_{E+G,1}$, $P_{E,2}$, and $P_{E+G,2}$. The symbol "P_E" and "P_{E+G}" represent the BRBF designs stemmed from the brace axial force demands (P), estimated from "E-Only" and "E+G" approaches, respectively. The number, 1 or 2, in the subscript respectively indicates that "1x" or "2x" local gravity load is considered for the BRBF design.

Member sizes for models $P_{E,1}$ and $PE_{,1(NLG)}$ are identical, being based on the same simplified design analysis in which the braces resist 100% of the tributary seismic load and none of the gravity load. (Similarly, models $P_{E,2}$ and $P_{E,2(NLG)}$ are identical.) The subscript "NLG" refers only to the modelling of gravity loads in the NLRHA used to assess performance. In the "NLG" case, all gravity loads, including those tributary to the frame, are placed on the leaning column.

It is noted that, as illustrated in Figure 2, the frames in each of the four design cases resists one-quarter of the total seismic load. This is accomplished by modelling a leaning column which carries the gravity load of

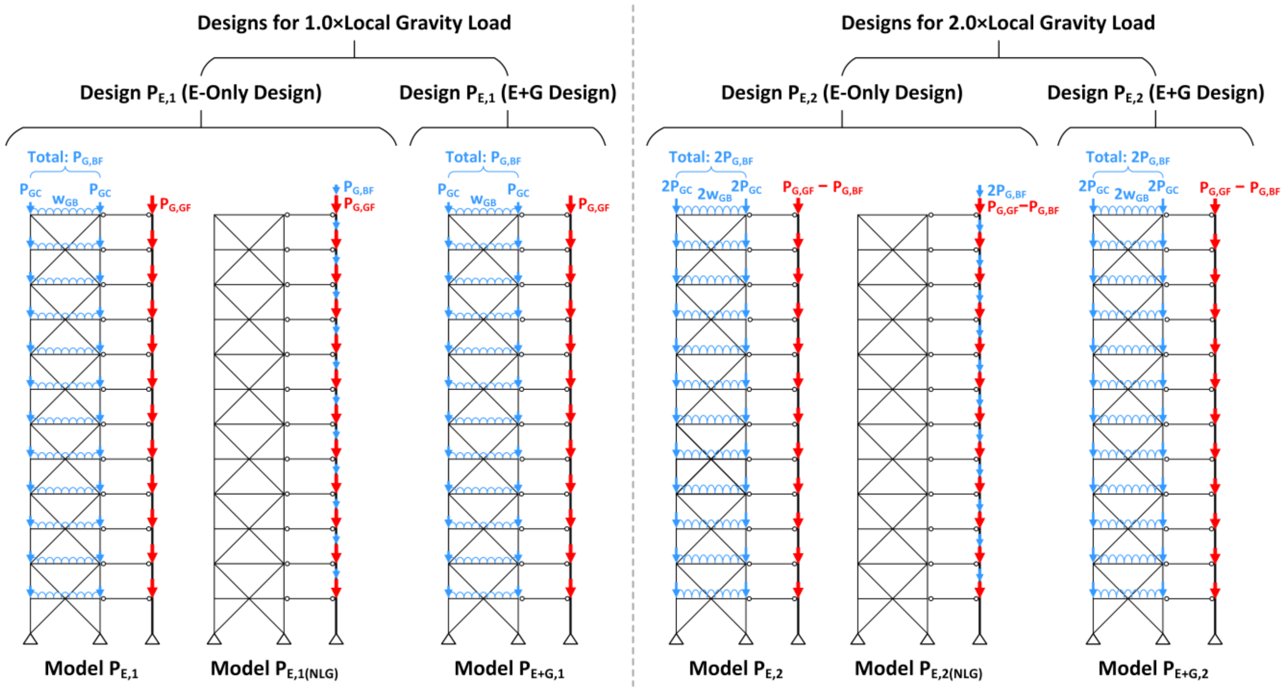

Figure 2: Four design cases and six models considered in this study.

the original NIST building that is tributary, for lateral design, to that frame. The total gravity load applied on the BRBF together with its associated gravity system are identical for the four design cases. In other words, the four BRBF design cases in this study were designed for the same seismic weights but with different proportioning to the frame columns versus the leaning column.

Table 1 summarizes the results of the four BRBF designs. Member sizes and key demand-to-capacity ratios (DCRs) are reported. The commercially available software ETABS (CSI, 2019) was employed to conduct the analyses for brace sizing. Three-dimensional ETBAS frame models, using the same geometries of the 12-story NIST building, were constructed to represent the four design cases. In addition to static analyses solving for the gravity load effects, an Equivalent Lateral Force (ELF) analysis (ASCE, 2022) and a Response Spectrum Analysis (RSA) were performed on these ETABS models. It is noted that, in this study, the sizing of BRBs was determined by the load effects associated with RSA. The brace design DCRs regarding ELF analyses were tabulated in Table 1 for comparison purpose but were not considered for sizing braces. Furthermore, in BRB sizing, the steel core areas were rounded up to the nearest 0.5 in² precision; and the minimum yield stress of A36 steel core, $F_{ysc,min}$, is taken as 262 MPa (38 ksi) , while the maximum yield stress is used for calculating frame member demands as will be discussed later.

Table 1: BRBF design summaries

(a) Desing for 1.0 Local Gravity Load

Level / Story	"E-Only" Design (Design $P_{E,1}$)							"E+G" Design (Design $P_{E+G,1}$)						
	BRB			Column		Beam	Story Drift	BRB			Column		Beam	Story Drift
	A_{sc} (mm²x10³)	DCR_{ELF}[1]	DCR_{RSA}[2]	Shape	DCR	Shape	$C_d\theta_E$ (rad.)	A_{sc} (mm²x10³)	DCR_{ELF+G}[3]	DCR_{RSA+G}[4]	Shape	DCR	Shape	$C_d\theta_E$ (rad.)
12	1.0	0.588	0.850	W12×40	0.422	W18×76	1.66%	1.0	0.578	0.882	W12×40	0.422	W18×76	1.52%
11	1.6	0.746	0.848	W12×40	0.682	W21×62	1.74%	1.9	0.902	0.975	W12×40	0.677	W21×62	1.49%
10	1.6	1.078	0.962	W14×68	0.802	W18×76	1.87%	2.3	0.854	0.795	W14×74	0.827	W18×76	1.52%
9	1.9	1.128	0.932	W14×68	0.922	W21×62	1.70%	2.6	1.168	0.997	W14×74	0.935	W21×62	1.36%
8	1.9	1.314	0.921	W14×109	0.743	W18×76	1.71%	2.9	0.987	0.764	W14×109	0.890	W18×76	1.33%
7	2.3	1.251	0.926	W14×109	0.803	W21×62	1.51%	3.2	1.213	0.946	W14×109	0.950	W21×62	1.14%
6	2.3	1.347	0.913	W14×132	0.922	W18×76	1.48%	3.2	1.042	0.803	W14×159	0.927	W18×76	1.12%
5	2.6	1.239	0.962	W14×132	0.971	W21×62	1.23%	3.5	1.233	0.993	W14×159	0.967	W21×62	0.94%
4	2.9	1.137	0.868	W14×176	0.939	W18×76	1.16%	3.9	0.940	0.807	W14×233	0.878	W18×76	0.89%
3	3.2	1.043	0.935	W14×176	0.975	W21×62	0.95%	4.2	1.109	0.992	W14×233	0.905	W21×62	0.73%
2	3.5	0.957	0.873	W14×233	0.939	W18×76	0.87%	4.5	0.837	0.832	W14×283	0.952	W18×76	0.69%
1	3.5	0.959	0.988	W14×233	0.966	W21×62	0.71%	4.8	1.007	0.961	W14×283	0.974	W21×62	0.52%

(b) Desing for 2.0 Local Gravity Load

Level / Story	"E-Only" Desing (Design $P_{E,2}$)							"E+G" Design ($P_{E+G,2}$)						
	BRB			Column		Beam	Story Drift	BRB			Column		Beam	Story Drift
	A_{sc} (mm²x10³)	DCR_{ELF}[1]	DCR_{RSA}[2]	Shape	DCR	Shape	$C_d\theta_E$ (rad.)	A_{sc} (mm²x10³)	DCR_{ELF+G}[3]	DCR_{RSA+G}[4]	Shape	DCR	Shape	$C_d\theta_E$ (rad.)
12	1.0	0.588	0.824	W14×48	0.512	W18×76	1.36%	1.3	0.456	0.684	W14×48	0.564	W18×76	1.17%
11	1.6	0.746	0.839	W14×48	0.956	W21×62	1.45%	2.6	0.911	0.961	W14×48	0.993	W21×62	1.08%
10	1.6	1.078	0.975	W14×109	0.566	W18×76	1.59%	2.6	0.793	0.750	W14×109	0.692	W18×76	1.15%
9	1.9	1.128	0.958	W14×109	0.688	W21×62	1.49%	3.5	1.053	0.936	W14×109	0.811	W21×62	1.00%
8	1.9	1.314	0.954	W14×132	0.847	W18×76	1.50%	3.5	0.874	0.698	W14×159	0.900	W18×76	1.00%
7	2.3	1.251	0.960	W14×132	0.946	W21×62	1.33%	3.9	1.212	0.997	W14×159	0.981	W21×62	0.87%
6	2.3	1.347	0.947	W14×193	0.840	W18×76	1.31%	3.9	0.944	0.748	W14×233	0.924	W18×76	0.86%
5	2.6	1.239	0.985	W14×193	0.906	W21×62	1.12%	4.5	1.163	0.987	W14×233	0.979	W21×62	0.73%
4	2.9	1.137	0.891	W14×257	0.857	W18×76	1.05%	4.5	0.896	0.790	W14×311	0.948	W18×76	0.71%
3	3.2	1.043	0.941	W14×257	0.906	W21×62	0.90%	5.5	1.047	0.963	W14×311	0.988	W21×62	0.55%
2	3.5	0.957	0.883	W14×311	0.920	W18×76	0.83%	5.5	0.774	0.770	W14×398	0.969	W18×76	0.54%
1	3.5	0.959	0.985	W14×311	0.961	W21×62	0.71%	5.8	1.011	0.992	W14×398	1.001	W21×62	0.41%

[1]Brace DCR determined from an Equivalent Lateral Force (ELF) analysis assuming braces take all seismic effect and neglecting gravity load effect
[2]Brace DCR determined from a response spectrum analysis (RSA) considering earthquake effect only
[3]Brace DCR determined from the load combination of the earthquake effect from ELF analysis and the gravity load effect from $(1.2+0.2S_{DS})D+0.5L$
[4]Brace DCR determined from the load combination of the earthquake effect from RSA and the gravity load effect from $(1.2+0.2S_{DS})D+0.5L$

For the "E-Only" design cases (i.e., Designs $P_{E,1}$ and $P_{E,2}$), the BRBs were sized for the force demand obtained from RSA only without considering gravity loads that might otherwise be taken by the braces due to their stiffness. The associated brace design DCR is denoted as DCR_{RSA}. As shown in Table 1, the BRB sizes for these two design cases ($P_{E,1}$ and $P_{E,2}$) are the same but the DCR_{RSA} values are slightly different. This is because different local gravity loads on the frame were considered so that the BRBF column sizes are different for the two cases (the BRBF columns in PE,2 are generally larger than those in PE,1), which results in differences in the dynamic properties (the structural period of PE,2 is shorter than those of PE,1) and therefore in the RSA results between the two design cases. In addition, the brace design DCRs considering the ELF effect only, denoted as DCRELF, for these two cases are also listed in Table 1. The DCR_{ELF} values (many of which are even greater than 1.0) are generally larger than the DCR_{RSA} values for both cases, suggesting that the RSA would lead to a more economical design than ELF method for the 12-story BRBF building considered in this study. The fact that the DCR_{RSA} values are smaller than the DCR_{ELF} values and that they are also closer to 1.0 indicates that efficient brace sizing is achieved for the two cases using the RSA analysis method. For this reason (that the RSA resulted in lighter braces) and because RSA is used more commonly for the design of taller BRBF structures, it was desirable to base the design on the RSA brace sizes rather than having the relatively stronger design that would be associated with the ELF design.

For the E+G design cases (i.e., Designs $P_{E+G,1}$ and $P_{E+G,2}$), the BRB sizes were determined for a load combination of the RSA result and the gravity load effect of $(1.2+0.2S_{DS})\cdot D+0.5L$, with a corresponding DCR denoted as DCR_{RSA+G} listed in Table 1. It can be found from Table 1, that the BRB sizes in the E+G design cases are always larger than those in the E-Only design cases except at the roof level where they are the same. As the local gravity load increased, larger braces resulted in the E+G design approach. For comparison purpose, the DCR values with respect to a load combination of the ELF analysis and gravity load effect, denoted as DCR_{ELF+G}, are tabulated in Table 1. Similar to results of E-only design, the DCR_{ELF+G} values are generally greater than the DCR_{RSA+G} values for the two E+G design cases, implying again a more efficient design for using RSA method.

Accompanying the sizing of BRB yielding core area, the detailing of braces was conducted for the typical CoreBrace bolted type BRBs to determine the associated stiffness modification factors, KF, and overstrength factors for the BRBs as provided in Table 2. In accordance with AISC 341-22 (AISC, 2022), the overstrength factors, ω and β, were determined from the backbone curves of the AISC qualification tests for BRBs at the core strain associated with the greater of a story drift ratio of 2% and 2 times the design story drift (taken as a brace deformation of $2\cdot C_d\cdot \Delta y$, where $C_d = 5$ is the deflection amplification factor for BRBF and Δy is the brace deformation at the initial yielding). For all design cases in this study, the 2% story drift requirement controlled the determination of overstrength factors. Factors were selected based on CoreBrace qualification tests for similar sized braces.

For all design cases, the BRBF columns were sized via the capacity-limited design that considers the column axial force demands based on the expected brace axial forces (i.e., the adjusted brace strength). The adjusted brace strength in tension and compression, denoted as $P_{u,T}$ and $P_{u,C}$, respectively, are determined from:

$$P_{u,T} = \omega F_{ysc,max} A_{sc} \tag{1}$$

$$P_{u,C} = \beta\omega F_{ysc,max} A_{sc} \tag{2}$$

where $F_{ysc,max}$ = 317 MPa (46 ksi) is the max allowable value of the yielding core material strength. Column design results are listed in Table 1. The tabulated DCRs were determined from the column axial force demands under the load combination of $(1.2+0.2S_{DS})\cdot D+0.5L+E_{cl}$, where E_{cl} is the capacity-limited horizontal seismic load effect. RAM Structural System (Bentley Systems, Inc., 2022) was used to confirm these column design DCRs. As the brace sizes were increased, higher axial force demands must be considered in design of BRBF column. It is clear from Table 1, that the E+G design method, in which the larger braces are sized would result in heavier columns than the E+G design approach. Table 3 shows the DCRs of the BRBF columns for axial force demand induced by the combined gravity and vertical earthquake effects (named G+E_v effect), denoted as DCR_{G+Ev}, for the four design cases. For the 1x local gravity load cases ($P_{E,1}$ and $P_{E+G,1}$), representing the perimeter BRBFs, the BRBF columns use about 33% of their capacity to resist the G+Ev effect, while this ratio for the 2x local gravity load cases ($P_{E,2}$ and $P_{E+G,2}$), representing the interior BRBFs, is about 45%. Although the BRB sizes are the same for Designs $P_{E,1}$ and $P_{E,2}$, which means that the part of column axial force demands induced by the adjusted brace forces are identical, with a local gravity load twice than Design $P_{E,1}$ requires the BRBF columns in $P_{E,2}$ to be larger.

Table 2: BRBF sizes and design parameters

(a) Desing for 1.0 Local Gravity Load

Story	"E-Only" Design (Design $P_{E,1}$)						"E+G" Design (Design $P_{E+G,1}$)					
	A_{sc} (mm^{2}x10^3)	L_{ysc} (mm)	ε_{BRB}* (mm/mm)	KF	ω	ωβ	A_{sc} (mm^{2}x10^3)	L_{ysc} (mm)	ε_{BRB}* (mm/mm)	KF	ω	ωβ
12	1.0	3373	1.93%	1.56	1.37	1.58	1.0	3373	1.93%	1.56	1.37	1.58
11	1.6	4346	1.50%	1.33	1.29	1.44	1.9	4316	1.51%	1.33	1.29	1.44
10	1.6	4414	1.47%	1.32	1.29	1.44	2.3	4346	1.50%	1.33	1.29	1.44
9	1.9	4316	1.51%	1.33	1.29	1.44	2.6	4090	1.59%	1.40	1.31	1.48
8	1.9	4384	1.48%	1.32	1.29	1.44	2.9	4206	1.54%	1.35	1.30	1.47
7	2.3	4279	1.52%	1.33	1.30	1.46	3.2	4136	1.57%	1.37	1.31	1.48
6	2.3	4346	1.50%	1.33	1.29	1.44	3.2	4204	1.55%	1.39	1.30	1.47
5	2.6	4091	1.59%	1.40	1.31	1.48	3.5	4059	1.60%	1.40	1.31	1.48
4	2.9	4205	1.55%	1.35	1.30	1.47	3.9	4009	1.62%	1.42	1.32	1.49
3	3.2	4137	1.57%	1.37	1.31	1.48	4.2	3917	1.66%	1.43	1.32	1.49
2	3.5	4124	1.58%	1.39	1.31	1.48	4.5	3951	1.64%	1.42	1.32	1.49
1	3.5	4101	1.58%	1.39	1.31	1.48	4.8	3892	1.67%	1.42	1.32	1.49

(b) Desing for 2.0 Local Gravity Load

Story	"E-Only" Desing (Design $P_{E,2}$)						"E+G" Design ($P_{E+G,2}$)					
	A_{sc} (mm^{2}x10^3)	L_{ysc} (mm)	ε_{BRB}* (mm/mm)	KF	ω	ωβ	A_{sc} (mm^{2}x10^3)	L_{ysc} (mm)	ε_{BRB}* (mm/mm)	KF	ω	ωβ
12	1.0	3373	1.93%	1.56	1.37	1.58	1.3	4423	1.47%	1.33	1.29	1.44
11	1.6	4346	1.50%	1.33	1.29	1.44	2.6	4090	1.59%	1.40	1.31	1.48
10	1.6	4403	1.48%	1.32	1.29	1.44	2.6	4157	1.56%	1.39	1.31	1.48
9	1.9	4316	1.51%	1.33	1.29	1.44	3.5	4058	1.60%	1.40	1.31	1.48
8	1.9	4384	1.48%	1.32	1.29	1.44	3.5	4125	1.58%	1.39	1.30	1.47
7	2.3	4279	1.52%	1.33	1.30	1.46	3.9	3943	1.65%	1.42	1.32	1.49
6	2.3	4346	1.50%	1.33	1.29	1.44	3.9	4010	1.62%	1.42	1.32	1.49
5	2.6	4091	1.59%	1.40	1.31	1.48	4.5	3900	1.67%	1.42	1.32	1.49
4	2.9	4205	1.55%	1.35	1.30	1.47	4.5	3966	1.64%	1.41	1.32	1.49
3	3.2	4137	1.57%	1.37	1.31	1.48	5.5	3664	1.77%	1.48	1.34	1.53
2	3.5	4124	1.58%	1.39	1.31	1.48	5.5	3715	1.75%	1.47	1.34	1.53
1	3.5	4082	1.59%	1.39	1.31	1.48	5.8	3634	1.79%	1.48	1.34	1.53

*BRB core strain resulted from the controlling brace deformation corresponding to 2% story drift

Table 3: Column demand-to-capacity ratios for gravity load effect

Story	Design for 1.0 Local Gravity Load					Design for 2.0 Local Gravity Load				
		Design $P_{E,1}$		Design $P_{E+G,1}$			Design $P_{E,2}$		Design $P_{E+G,2}$	
	P_{G+Ev} (kN)	Column Shape	DCR_{G+Ev}*	Column Shape	DCR_{G+Ev}*	P_{G+Ev} (kN)	Column Shape	DCR_{G+Ev}*	Column Shape	DCR_{G+Ev}*
12	229	W12×40	0.18	W12×40	0.18	458	W14×48	0.31	W14×48	0.31
11	559	W12×40	0.45	W12×40	0.45	1118	W14×48	0.76	W14×48	0.76
10	889	W14×68	0.33	W14×74	0.30	1779	W14×109	0.33	W14×109	0.33
9	1220	W14×68	0.45	W14×74	0.41	2439	W14×109	0.45	W14×109	0.45
8	1550	W14×109	0.32	W14×109	0.29	3100	W14×132	0.47	W14×159	0.39
7	1880	W14×109	0.38	W14×109	0.35	3760	W14×132	0.57	W14×159	0.47
6	2210	W14×132	0.34	W14×159	0.27	4421	W14×193	0.45	W14×233	0.37
5	2541	W14×132	0.39	W14×159	0.32	5082	W14×193	0.52	W14×233	0.43
4	2871	W14×176	0.32	W14×233	0.24	5742	W14×257	0.44	W14×311	0.36
3	3201	W14×176	0.36	W14×233	0.27	6403	W14×257	0.49	W14×311	0.40
2	3532	W14×233	0.30	W14×283	0.24	7063	W14×311	0.44	W14×398	0.34
1	3862	W14×233	0.32	W14×283	0.27	7724	W14×311	0.48	W14×398	0.38
		Avg. =	0.34	Avg. =	0.30		Avg. =	0.48	Avg. =	0.41

*$DCR_{G+Ev} = [(1.2+0.2S_{DS})P_D+0.5P_L]/\varphi_c P_n$

The BRBF beam design considered the axial and flexural force demands in the beam induced by the adjusted strengths of the adjacent braces in combination with the gravity load effect. Identical beam sizes were selected for the four design cases as listed in Table 1. Slightly oversized beam sections were selected to avoid the forming of plastic hinges within the beam span even when the beam force demand exceeds the expected design values due to the intensive shaking or higher-mode effect in the high-rise building during severe earthquakes. As the BRBF beams are assumed to be pin-ended in this study, the oversizing of beams would not significantly increase lateral stiffness and, as such, should not distort the NLRHA results.

In addition to the strength checks for BRBF, story drift checks were conducted to ensure that the lateral stiffness of BRBF was adequate to meet code requirements. The elastic story drift angle, θ_E, was determined from an RSA with a base shear scaled to be the same as the drift-check ELF analysis by using ETABS. As shown in Table 1, the design story drifts, estimated as $C_d\theta_E$, are less than the code-prescribed allowable story drift angle of 0.02 rad. (ASCE, 2022) for all design cases.

3 MODELLING FOR NONLINEAR RESPONSE HISTORY ANALYSIS

3.1 Analysis models

As shown in Figure 1, six two-dimensional frame models were developed in this study for NLRHA investigations into the gravity load effect on the BRBF seismic design. Each model is composed of a BRBF and a leaning column representing the P-Delta and lateral effects of the part of gravity frame system (1/4 of the NIST building) carried by the BRBF. Four of the models, Models $P_{E,1}$, $P_{E+G,1}$, $P_{E,2}$, and $P_{E+G,2}$, named after the four design cases, directly represent the four design cases, respectively. In these four models, the BRBF is subjected to the local gravity loads that are allocated to the BRBF while the leaning column carries the gravity loads tributary to the gravity system. Note that the BRBs in these four models are subjected to gravity loads in the analysis based on the relative rigidity between the BRBs and the frame members in the BRBF (though the BRB are sized accounting for this gravity in only the $P_{E+G,1}$ and $P_{E+G,2}$ models). Two additional models, named $P_{E,1(NLG)}$ and $P_{E,2(NLG)}$, were developed to represent a fictitious case for the E-Only design cases $P_{E,1}$ and $P_{E,2}$, respectively, where there was no local gravity load present on the frame. The subscript “NLG” in the model’s name indicates “No Local Gravity” as the frame in the model carries no local gravity loads and all the local gravity loads originally allocated to the BRBF are shifted to the leaning column (i.e., the leaning column carries the entire gravity load of 1/4 NIST building). Thus the BRBs in this model are not subjected to any gravity loads. The “NLG” models are included in this study to investigate the effect of the presence of the local gravity loads in BRBF on the seismic performance of the entire structure by comparing the NLRHA results of NLG models with their counterparts (e.g., Model $P_{E,1(NLG)}$ versus Model $P_{E,1}$). It is worth noting that, the seismic masses as well as the total gravity load carried by all 6 models are identical but the allocation of the gravity loads between the BRBF and the leaning columns changes. The six analysis cases considered are summarized in Table 4.

Table 4: Analysis Matrix

<table>
<tr><th colspan="2" rowspan="2"></th><th colspan="2">Gravity Present</th></tr>
<tr><th>Yes</th><th>No</th></tr>
<tr><td rowspan="2">Braces Sized for Gravity</td><td>Yes</td><td>$P_{E+G,1}$
$P_{E+G,2}$</td><td>-</td></tr>
<tr><td>No</td><td>$P_{E,1}$
$P_{E,2}$</td><td>$P_{E,1(NLG)}$
$P_{E,2(NLG)}$</td></tr>
</table>

3.2 Nonlienar modelling details

Nonlinear models were developed using the *OpenSees* analysis platform (McKenna et al., 2010). Models were created in two-dimensions including a single bay BRBF and a fishbone system (Lignos et al. 2013) that includes the resistance of gravity beam-to-column connections and acts as a leaning (i.e., P-Delta) column. Beam-to-column connections within the BRBF frame were modelled as pinned (i.e., no moment-resisting connections). All column base connections were also modelled as pinned. An illustration of the different components of the model are given in Figure 3. Offset elements were used in the braced frame to model the stiffened regions inside of panel zones and locations of gusset connections. Offsets assume ten times the elastic flexural properties of the members framing into centerline nodes.

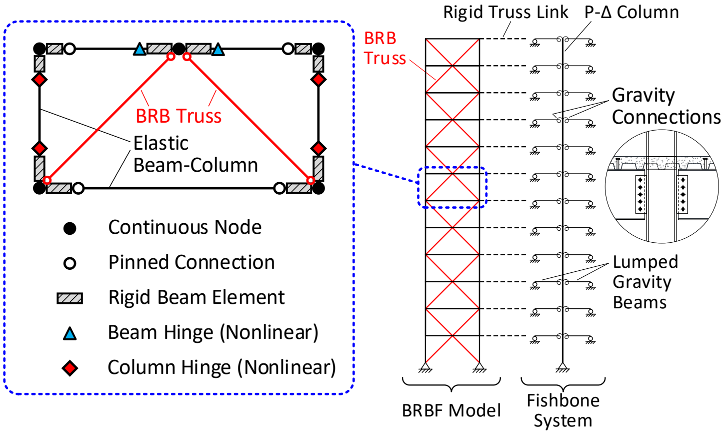

Figure 3: Illustration of OpenSees model used for nonlinear response history analysis

Buckling restrained braces (BRBs) were modelled as corotational truss elements (using the workpoint-to-workpoint length, L_{wp}) with a hysteretic behavior defined by a Menegatto-Pinto steel material (SteelMPF) with isotropic strain hardening. Initial stiffness of the BRBs was defined by the effective stiffness factor, KF (see Table 3) using the bay geometry and the L_{wp}. Cyclic properties of BRBs were calibrated using the AISC 341 loading protocol (section K3.4c of AISC, 2022). BRB material parameters were calibrated to obtain the ultimate strength for both tension (P_{ut}) and compression (P_{uc}) at the required stroke, which is taken as the brace deformation corresponding to a 2% story drift ratio (see Figure 4).

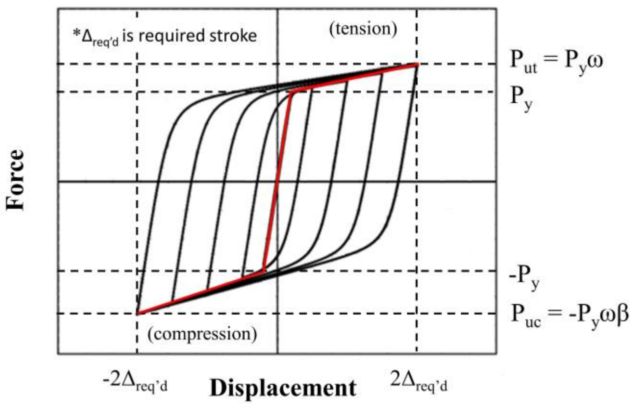

Figure 4: Example calibration of a BRB material

BRBF column hinges were included in the model outside of assumed gusset and panel zone regions using the BiLin (*Modified Bilinear IMK*; Ibarra et al. 2005) hysteretic material model in *OpenSees* with properties calculated according to the ATC-114/NIST modelling guidelines (NIST, 2017). BRBF beam hinges were placed outside of the central gusset regions (i.e., not at beam-to-column connections, which were pinned) using the BiLin material and input parameters developed by Lignos and Krawinkler (2011).

Resistance provided by simple gravity connections (within fishbone frame shown in Figure 3) was modelled using nonlinear hinges representing the lumped properties of shear tab connections in the part of gravity frame carried by the BRBF considered. The gravity connections were modelled using the *Pinching4* material (Lowes et al., 2003) with parameters calculated according to ATC-114/NIST guidelines (NIST, 2017; Liu and Asteneh-Asl, 2000, 2004).

Models include second order (P-Delta) effects both locally on the braced frame and through the leaning column as part of the fishbone gravity framing model. Inherent viscous damping is included in the models as 2% Rayleigh damping applied to the first and third modes of vibration. Mass proportional damping is applied to all nodes within the model. Initial stiffness proportional damping was only applied to linear elastic elements in the model. The stiffness of nonlinear frame hinges, connecting elastic elements, and stiffness proportional damping coefficients are adjusted in line with the recommendations of Zareian and Medina (2010) for inelastic planar structures.

3.3 Ground motion input for nonlinear response history analysis

The BRBF archetype designs were analysed using 12 pairs of ground motion records (24 in total) selected from the FEMA P-695 far-field set (FEMA, 2009), which consists of 22 pairs of horizontal accelerograms (44 accelerograms total). The target spectral shape for scaling ground motions was the code-prescribed design spectrum (ASCE, 2022) with the spectral accelerations S_{DS} = 1.0 g and S_{D1} = 0.6 g (FEMA, 2009), which are consistent with those employed for the four design cases in this study. The intensity measure used for the study is the 5%-damped spectral acceleration at the averaged 1st-mode period ($T_{1,avg}$) of the *OpenSees* models for the four designs ($P_{E,1}$, $P_{E+G,1}$, $P_{E,2}$, and $P_{E+G,2}$). For selection of ground motions, the 22 pairs of horizontal accelerograms in the FEMA P-695 far-field set (called original ground motion set) were first individually scaled to the Maximum Considered Earthquake (MCE) level (ASCE, 2022). When a ground motion has at least one horizonal accelerogram requires an MCE scale factor outside the desirable scale factor range from 0.25 to 4.0 (ASCE, 2022), both horizontal accelerograms of that ground motion were removed from the original ground motion, which resulted in 12 pairs of ground motion records (24 in total) being selected. Each ground motion was scaled to both Design Basis Earthquake (DBE) and MCE levels. Figure 5 shows the response spectra of the scaled ground motions selected in this study compared with their corresponding target spectrum (MCE or DBE). It can be found that the median spectrum of the scaled ground motions well matches the target spectrum over a wide range of the period, suggesting the median NLRHA

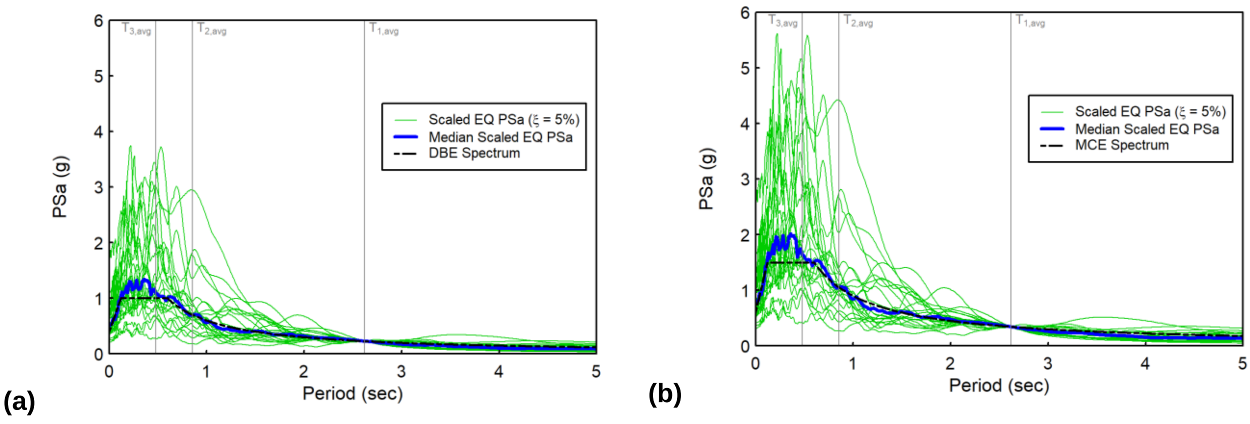

Figure 5: Response spectra of 24 selected ground motions for (a) DBE- and (b) MCE-scaled levels

response obtained for the selected ground motion set would desirably representing the BRBF seismic response. The study considered two analysis intensities corresponding to the DBE and MCE but will focus on the median responses at MCE intensity.

4 ANALYSIS RESULTS

The NLRHA results for the 6 OpenSees models are reported for the median of the peak responses from the ground motion set on story drift, residual drift, BRB normalized ultimate force, BRB strain, and column compressive force. If a significant effect exists regarding the sharing of gravity loads in BRBF design (and hence this sharing should be considered) then it is expected that the P_{E+G} and the P_{E+NLG} cases will show similar results. However, if the current design practice of ignoring the effect of the gravity load in the BRBs (E-only design philosophy) is acceptable, then it would be expected that each E-only design counterpart pair (i.e., the P_E and $P_{E(NLG)}$ cases) would show more similar results. In other words, if the case where local gravity load on BRBF is present, but ignored for BRB sizing (e.g., Model $P_{E,1}$), behaves similarly to the case where local gravity is not present on BRBF (e.g., Model $P_{E,1(NLG)}$), then the assumption that the gravity sharing can be ignored would be justified. However, if the case with gravity present and with the braces sized for gravity (P_{E+G}) were more similar to the case with gravity not present and the braces not sized for gravity (P_{E+NLG}) then it could be concluded that gravity sharing should be considered, and the braces should be designed for that load. Results are provided primarily for the MCE intensity level.

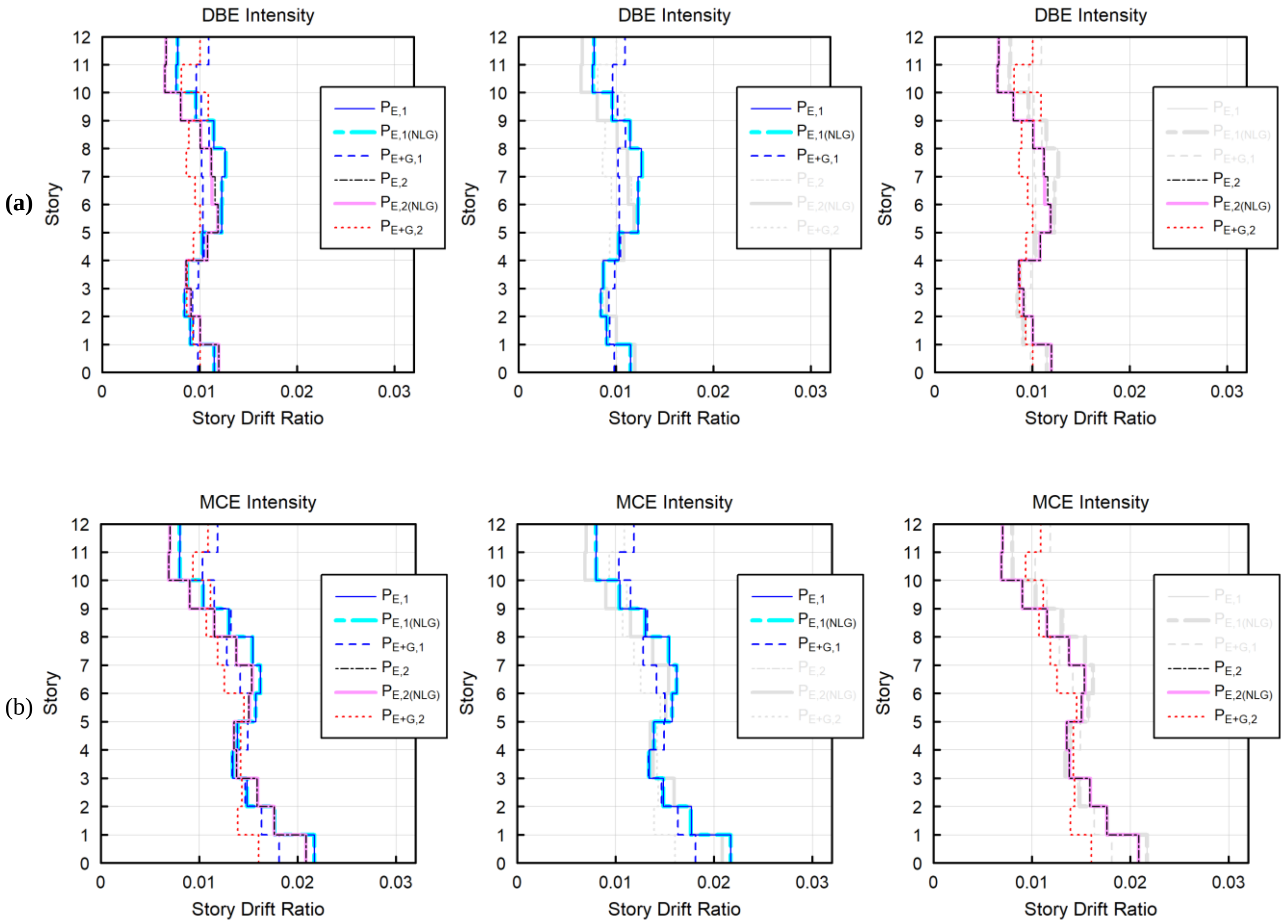

Figure 6: Story drift ratio at (a) DBE and (b) MCE levels

4.1 Story drift ratio

DBE and MCE story drift profiles of the structure are shown in Figures 6(a) and 6(b), respectively. The results indicate that the drift is somewhat greater at the top of the structure for the P_{E+G} case than for the P_E and $P_{E(NLG)}$ cases no matter how much (1x or 2x) local gravity load on BRBF is considered, however at the lower two levels of the structure the P_{E+G} case has a lower drift. This lower drift at the base of the structure in the P_{E+G} case is consistent with having the stiffer braces that resulted from sizing them for the additional gravity load, or from oversizing them for any other reason. More importantly, the trends of the P_E and $P_{E(NLG)}$ cases follow each closely and are nearly identical while the P_{E+G} is clearly different among each local gravity load group. It appears that the 2x local gravity cases, in general, have smaller MCE drifts the 1x local gravity cases. This is because the 2x local gravity design cases possess larger member sizes. While the first-story MCE drifts in the four E-only design Models $P_{E,1}$, $P_{E,1(NLG)}$, $P_{E,2}$, and $P_{E,2(NLG)}$, which are about 2.17%, 2.17%, 2.08%, and 2.09% respectively, slightly exceed the code allowable of 2% [see Fig. 6(b)], it should be noted that the MCE intensity is being compared. For the DBE intensity [see Fig. 6(a)], the story drift responses for all six models do not exceed 2% at any level, indicating the code requirement is both satisfied and valid if available BRB stroke should not be exceeded in MCE events. It can be noted also that the design story drift ratios reported in Table 1 are generally conservative except at lower levels where the NLRHA results give slightly higher values (but in all cases less than the allowable, as noted).

4.2 Residual story drift ratio

Residual drift is the permanent drift remaining after a seismic event. This is calculated by obtaining the final displaced shape of the structure following the free vibration response duration after each earthquake excitation. An additional ten seconds of analysis time was added in order to reliably allow the structure to be damped out during free vibration (noting that no dynamic collapses were obtained at the intensity levels considered). Plots of residual drift, at DBE and MCE intensities, are shown in Figure 7(a) and (b) respectively. The trends follow those of the story drift ratio with the P_E and $P_{E(NLG)}$ cases matching each other closely while the P_{E+G} is clearly different.

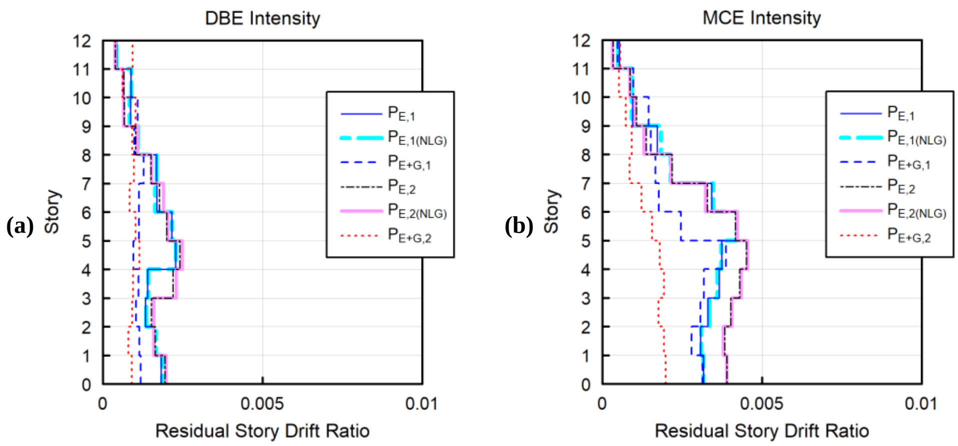

Figure 7: Residual story drift ratio at (a) DBE and (b) MCE levels

4.3 BRB Normalized force and strain

BRB normalized ultimate force represents the ratio of the maximum force in the BRB to its yield force, a measure of the overstrength seen in the BRB. A plot of the BRB normalized force is provided in Figure 8. BRBs were modelled as having an expected yield strength, $F_{ysc,exp}$ of 290 MPa (42 ksi), and as such, this normalized force is only a measure of the strain hardening and compression overstrength that develops and does not include the material overstrength that would be considered when a material yield stress range ($F_{ysc,min}$ to $F_{ysc,max}$) is allowed for (the equivalent of allowing for an R_y). A similar trend is seen here with the P_E and $P_{E(NLG)}$ cases matching each other closely, though with slightly more deviation than seen previously. Figure 8(a) shows that the analytical overstrength at MCE in the first story of E-only design cases only slightly exceeded the design overstrength ($\omega\beta$) values in Table 2 (by about 4.5% and 3.6% for Models $P_{E,1}$ and $P_{E,2,}$ respectively), which is consistent with the fact that the overstrength factors were determined for the 2% story drift deformation level but the first-story MCE drifts slightly exceeded 2%. However, the design cumulative overstrength demands on the column ($Fy \cdot Asc \cdot \omega\beta$) is considerably less than the MCE results. As such, even though the design values are at DBE level, they are, in fact, quite adequate for MCE design.

Plots of BRB strain at MCE are shown in Figure 8(b). As with the other figures in the study, there is a similar trend in the P_E and $P_{E(NLG)}$ cases and a difference between these two and the $P_{(E+G)}$ case. Only the BRB strains in the first story of E-only design cases slightly exceed the design values (by about 8.7% and 4.7% for Models $P_{E,1}$ and $P_{E,2}$, respectively) shown in Table 2 (determined in accordance with ASCE 341-16). The higher strains at this level remain, however, within tested values (which typically achieve at least 3% strain) and it is noted again that the strains in Table 2 are calculated at DBE intensities and yet are satisfactory for MCE demands.

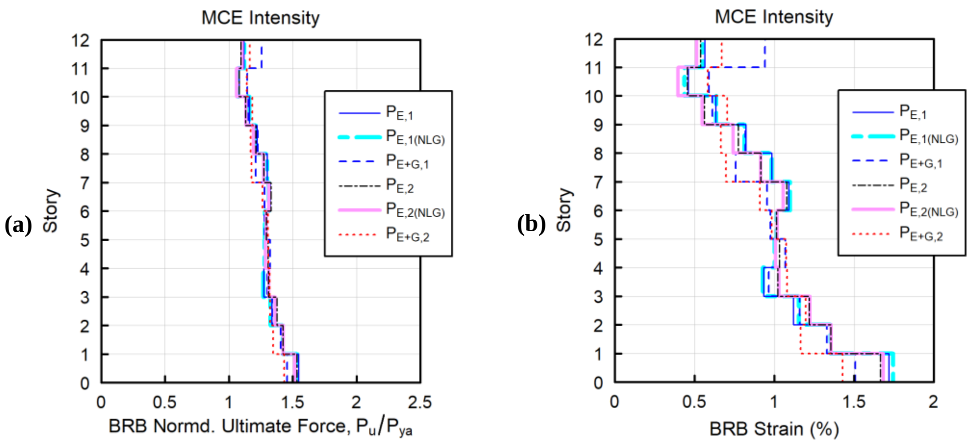

Figure 8: BRB responses at MCE: (a) BRB normalized ultimate force; (b) BRB strain

4.4 Column compression axial force

The final parameters considered are the column compressive load and column DCR as shown in Figure 9(a) and 9(b). The absence of gravity load is clearly seen in the $P_{E(NLG)}$ cases where load is only added to the columns at the beam-column intersections and not at the X-intersection levels. The P_E and P_{E+G} cases are similar, as would be expected since all vertical loads will ultimately reach the columns, but the $P_{E+G,}$ with its added stiffness, ultimately results in slightly more axial force in the column due to the stiffer (and higher capacity) braces developing a greater seismic resistance. All three cases shed more load into the columns at the beam-column intersections and in no case does the column compressive DCR exceed 0.75. These NLRHA DCRs, at MCE, are notably less than the elastic analysis DCRs reported in Table 1 suggesting conservatism in design methods.

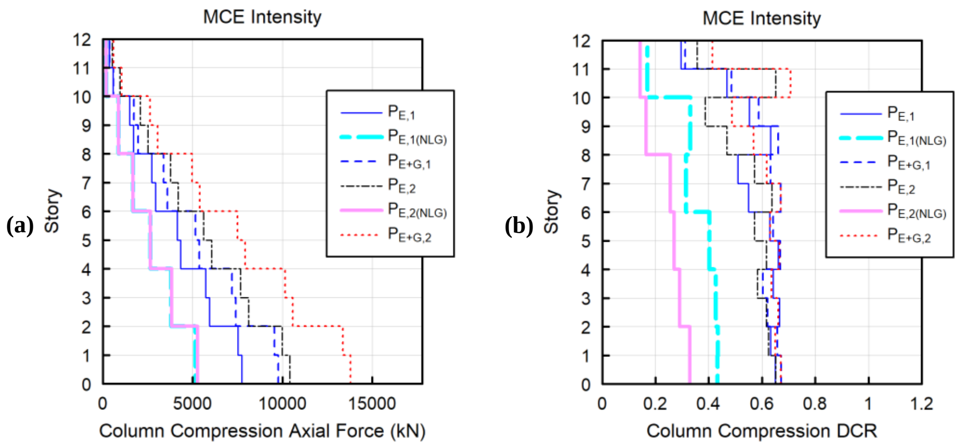

Figure 9: Column compression axial force (a) demand and (b) DCR at MCE level

5 CONCLUSIONS

A twelve-story building was considered for the cases where the BRBs in a perimeter frame were sized only for lateral loads (P_E), where they were sized for lateral loads plus the gravity loads allocated based on their stiffness (P_{E+G}), and for the case with no local gravity present ($P_{E(NLG)}$). The frame columns were sized economically, and the structure was subjected to 24 ground motions at both DBE and MCE intensities. Results, at MCE intensities, were presented for story drift, residual drift, BRB normalized ultimate force, BRB strain, column compressive force, and column compressive DCR, with additional results at DBE intensities presented for story drift, residual drift, and BRB strain. Results presented show that the P_E and $P_{E(NLG)}$ cases consistently had similar results, indicating that neglecting gravity loads in the BRB (even though they are present in the frame), behaved similarly to the analysis case where gravity loads are not present in the frame at all. Accounting for gravity loads in the BRB, as done in the P_{E+G} case, improved performance as would be expected of any measure, or penalty, that arbitrarily increased BRB sizes. The results did not change for the case where the vertical gravity load taken by the frame was doubled (as might be the case at an interior frame).

It should be noted that the application of any penalty that increases BRB size will have a beneficial effect on performance, regardless of whether such a penalty is necessary to counteract a detrimental condition. Two comparisons help establish whether there is a detrimental effect of gravity load in the BRBs and whether the "penalty" of designing the BRBs for the combined effect of gravity and seismic loads adequately compensates for the detrimental effect (if any). If there were such a detrimental effect of gravity load in the BRBs, one would expect the P_E case to have significantly greater response than the $P_{E(NLG)}$ case. If the penalty of designing the BRBs for the combined effect of gravity and seismic loads were both necessary (due to a detrimental effect) and adequate to compensate for the detrimental effect, one would expect the P_{E+G} case to have similar response to the $P_{E(NLG)}$ case. As can be seen in virtually every comparison, P_E and $P_{E(NLG)}$ have virtually identical responses, indicating that there is no detrimental effect requiring a penalty. Similarly, the fact that P_{E+G} typically has lower response than P_{E+NLG} suggests that designing BRBs for the combined effects is a greater penalty than is required.

Taken together, these two sets of comparisons suggest that no penalty is required to achieve the performance corresponding to the absence of gravity force in BRBs, and the current practice of neglecting the gravity load in BRBs is consistent with the expected performance of the system. The fact that P_{E+G} has lower response than P_E simply indicates that increasing BRB size results in lower response; this comparison does not shed light on the question of whether there is a detrimental effect and whether the penalty is necessary.

6 REFERENCES

AISC (2022). *Seismic Provisions for Structural Steel Buildings*, ANSI/AISC 341-22, American Institute of Steel Construction (AISC), Chicago, IL.

ASCE (2022). *Minimum Design Loads and Associated Criteria for Buildings and Other Structures*, ASCE/SEI 7-22, American Society of Civil Engineers (ASCE), Reston, VA.

Bentley Systems Inc. (2022). *RAM Structural System Manuals*, Bentley Systems Inc., Exton, PA.

CSI (2019). *CSI Analysis Reference Manual for SAP2000, ETABS, SAFE and CSiBridge*, ISO# GEN062708M1, Rev. 18, Computers & Structures, Inc. (CSI), Berkeley, CA.

FEMA (2009). *Quantification of Building Seismic Performance Factors*, FEMA P-695, Prepared by the Applied Technology Council for the Federal Emergency Management Agency (FEMA), Washington, D.C.

Ibarra, L.F., Medina, R.A., Krawinkler, H. (2005). Hysteretic Models that Incorporate Strength and Stiffness Deterioration, *Earthquake Engineering and Structural Dynamics*, 34(12): 1489-1511.

Lignos, D.G., Krawinkler, H. (2011). Deterioration Modeling of Steel Components in Support of Collapse Prediction of Steel Moment Frames under Earthquake Loading, *ASCE Journal of Structural Engineering,* 137(11): 1291-1302.

Lignos, D.G., Putman, C., Krawinkler, H. (2013). Seismic Assessment of Steel Moment Frames using Simplified Nonlinear Models, *Computational Methods in Earthquake Engineering*, *Computational Methods in Applied Sciences* book series, 30: 91-109.

Liu, J., Asteneh-Asl, A. (2000). Cyclic Testing of Simple Connections Including Effects of Slab, *ASCE Journal of Structural Engineering*, 126(1): 32-39.

Liu, J., Asteneh-Asl, A. (2004). Moment-Rotation Parameters for Composite Shear Tab Connections, *ASCE Journal of Structural Engineering*, 130(9): 1371-1380.

Lowes, L.N., Mitra, N., Altoonash, A. (2003). *A Beam-Column Joint Model for Simulating the Earthquake Response of Reinforced Concrete Frames*, Report No. 2003/10, Pacific Earthquake Engineering Research Center, University of California, Berkeley.

McKenna, F., Scott, M.H., Fenves, G.L. (2010). Nonlinear Finite-Element Analysis Software Architecture Using Object Composition, *ASCE Journal of Computing in Civil Engineering*, 24(1): 95-107.

NIST (2010). *Evaluation of the FEMA-P695 Methodology for Quantification of Building Seismic Performance Factors*, NIST GCR 10-917-8, Prepared by the NEHRP Consultants Joint Venture for the National Institute of Standards and Technology (NIST), Gaithersburg, MD.

NIST (2017). *Recommended Modeling Parameters and Acceptance Criteria for Nonlinear Analysis in Support of Seismic Evaluation, Retrofit and Design*, Report NIST GCR 17-917-45, Prepared by the Applied Technology Council for the National Institute of Standards and Technology (NIST), Gaithersburg, MD.

Saxey, B., Sabelli, R., Welch, D. (2021). Is Accounting for Gravity Loads in BRBF Design Necessary, *Proceedings, 2021 SEAOC Convention*, San Diego, CA.

Zareian, F., Medina, R.A. (2010) A Practical Method for Proper Modeling of Structural Damping in Inelastic Plane Structural Systems, *Computers and Structures*, 88(1-2): 45-53.